Mathematical Biosciences and Engineering

http://www.aimspress.com/journal/mbe

MBE, 20(2): 3342–3354.
DOI: 10.3934/mbe.2023157
Received: 17 October 2022
Revised: 25 November 2022
Accepted: 29 November 2022
Published: 05 December 2022

Research article

The SAITS epidemic spreading model and its combinational optimal suppression control

Wei Ding[1], **Li Ding**[1,*], **Zhengmin Kong**[1] **and Feng Liu**[2]

[1] School of Electrical Engineering and Automation, Wuhan University, Wuhan 430072, China
[2] School of Systems and Enterprises, Stevens Institute of Technology, Hoboken, NJ 07030, USA

* **Correspondence:** Email: liding@whu.edu.cn.

Abstract: In this paper, an SAITS epidemic model based on a single layer static network is proposed and investigated. This model considers a combinational suppression control strategy to suppress the spread of epidemics, which includes transferring more individuals to compartments with low infection rate and with high recovery rate. The basic reproduction number of this model is calculated and the disease-free and endemic equilibrium points are discussed. An optimal control problem is formulated to minimize the number of infections with limited resources. The suppression control strategy is investigated and a general expression for the optimal solution is given based on the Pontryagin's principle of extreme value. The validity of the theoretical results is verified by numerical simulations and Monte Carlo simulations.

Keywords: SAITS model; complex network; epidemic spreading; optimal control

1. Introduction

The Coronavirus Disease 2019 (COVID-19) has spread all over the world and endangered people's normal lives. For analyzing the dynamical process of epidemic spreading, it is of great significance to establish the mathematical model of disease propagation on complex networks. In the real world, the population can be considered homogeneous due to its extremely huge size [1]. Therefore, the population can be partitioned into different compartments according to different states of individuals. Since there is no difference in propagation dynamics between individuals within the same compartment, the process of epidemic spreading can be described as the transfer of individuals between compartments. Many scholars have proposed different compartment models to study the mechanism of epidemic spreading in the population, such as SIS [2], SIR [3, 4], SEIR [5], SVEIR [6], SEIRD [7], etc.

Since the spread of the disease will bring economic losses, crowd panic and other social instability,

scientists have analyzed the impact of different suppression methods on the spreading of epidemics. For example, isolating and treating individuals who are already infected [8], vaccinating individuals who are not infected [9, 10], controlling the movement of people [11] and requiring masks [12]. These suppression control strategies can be divided into two categories. One is to reduce the infection rate and the other is to increase the recovery rate.

The most popular way of reducing infection rates is vaccination. When individuals are vaccinated, their infection rate can be dramatically reduced, thereby inhibiting the spread of the disease. For instance, Shi et al. [13] proposed a class SIS model that integrates the effects of scenarios such as incomplete vaccination and incomplete immunization on disease transmission. The effect of isolation is similar to the vaccination. Ahuod S. Alsheri et al. [14] studied the effect of isolation rates on controlling the spread of COVID-19, using data given by the Ministry of Health of Saudi Arabia, and the result confirmed that early detection and isolation lead to a better control effect. The increase of recovery rates depends on government investment in the healthcare system and drug development, as well as the improvement of the individual's immunity and other related strategies.

It is worth noting that these strategies are always accompanied by some costs. Therefore, with limited resources, there is a strong need to develop optimal control strategies to suppress the widespread of epidemics at minimal cost. Many scholars have conducted relevant studies in this area. For example, Xu et al. [15] proposed a novel SIVRS mathematical model with viral variation and studied optimal control strategies for susceptible, infected and mutated individuals. Ana P. Lemos-Paião et al. [16] proposed a mathematical model of SIQR for treating cholera with quarantine, studied the model's disease-free and endemic equilibrium points and provided the optimal quarantine strategy to minimize the number of infectious individuals and costs. Laurent Miclo et al. [17] studied an setting with constrained ICU resources and high suppression costs. Results showed that the optimal control is discontinuous. Epidemics should be left unregulated initially, with a rapid social lockdown when approaching the ICU constraint, followed by gradual decontrol, and finally complete lifting of the regulation. Wu et al. [18] found that prevention and control measures such as isolation and vaccination can affect the accuracy of the model, and the accuracy is 6.7% higher when these factors are considered. Anuj Kumar et al. [19] proposed a nonlinear compartment model considering information-induced vaccination and treatment as two control strategies. The results showed that the execution of both strategies simultaneously was effective throughout the epidemic outbreak, while the execution of information-induced vaccination was effective only during the initial phase. G. Dimarco et al. [20] considered the heterogeneity described by the social contact of individuals and analysed the effects of introducing an optimal control strategy into the system, to limit selectively the mean number of contacts and reduce consequently the number of infected cases. The work most closely related to ours is [21], in which scholars have presented an optimal control problem on a SIR epidemic model including both vaccination and treatment control strategies on actual data, it has been demonstrated that using both control strategies simultaneously is more effective than using only one of the control strategies.

Among the previous works, few works considered the control strategy of reducing the infection rate and increasing the recovery rate simultaneously to suppress the spread of epidemics, while considering the control cost. However, in reality, the government and other relevant departments mostly take a two-pronged approach when dealing with infectious diseases, that is, informing the public to reduce travel, wear masks as well as get vaccination and medical treatment in time. Therefore, it is necessary to design an epidemic model that incorporates both types of control strategies to more accurately study

the effects of these suppression strategies on epidemic spreading.

Based on the above analysis, the main contents and contributions of this paper are as follows. Firstly, we propose a Susceptible-Alert-Infected-Treated-Susceptible (SAITS) epidemic model that incorporates a combinational control consisting of two types of strategies. One strategy is to get more individuals into the compartment with low infection rate, and the other is to get more individuals into the compartment with high recovery rate. The basic reproduction number of the model is calculated and the disease-free and endemic equilibrium points of the model are discussed. Secondly, the optimal control problem is investigated to minimize the cost of both infection and combinational suppression control, and a general expression of the optimal solution that reflects the trade-off between the infection cost and the combinational suppression control cost is obtained. Finally, to verify the theoretical results, Monte Carlo and numerical simulations are performed.

The rest of this paper is organized as follows. In Section 2, the SAITS epidemic model is developed. In Section 3, the basic reproduction number of the model and the disease-free and endemic equilibrium points are discussed. Meanwhile, an optimal control problem and its theoretical analysis is given. Monte Carlo and numerical simulations are performed to illustrate the results in Section 4. Conclusions are drawn in Section 5.

2. Model

Consider an undirected unweighted graph representing the relationship between individuals in a population, which consists of N nodes, with the connectivity between nodes represented by an adjacency matrix $A_{ij} = [a_{ij}] \in R^{N\times N}$, where $a_{ij} = 1$ means node i and node j are connected, conversely, $a_{ij} = 0$ means node i and node j are disconnected.

We propose an SAITS epidemic model in which individuals are divided into four compartments, namely, Susceptible (S), Alert (A), Infected (I) and Treated (T). Both the susceptible compartment S and the alert compartment A are collections of uninfected individuals. The infection rate of alert individuals is lower than susceptible individuals. Both the infected compartment I and the treated compartment T are collections of infected ones. The recovery rate of treated individuals is higher than infected ones.

A susceptible individual S or an alert individual A will become infected at the infection rate β_1 or $\beta_2(0 < \beta_1 < \beta_2 < 1)$, respectively, if they come into contact with an infected individual I. An infected individual I or a treated individual T will return to the susceptible state at the recovery rate r or $\lambda(0 < \lambda < r < 1)$, respectively. We believe that a susceptible individual will only enter the alert state if there is at least one infected individual in its neighborhood and itself is not infected next, an alert individual will not spread this awareness to other susceptible individuals, and the treated individual is not infectious.

We investigate a combinational suppression control strategy aimed at reducing infection rate and increasing recovery rate by transferring more individuals from compartment S to compartment A, while transferring more individuals from compartment I to compartment T. Under this strategy, a susceptible individual S will enter the alert state A with a probability of $u_1(0 < u_1 < 1)$ and an infected individual will enter the treated state T with a probability of $u_2(0 < u_2 < 1)$. The value of u_1 and u_2 reflects the strength of control strategy. The larger the value, the stronger the control effect. The flow chart of epidemic spreading is shown in Figure 1.

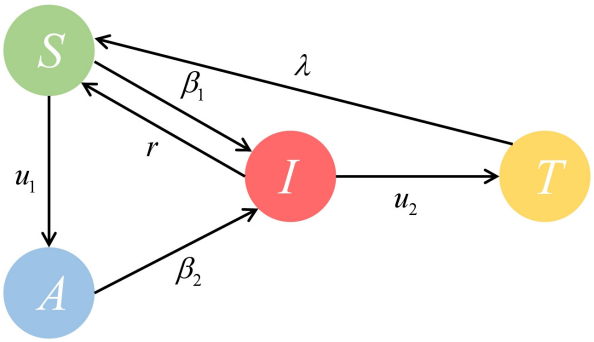

Figure 1. The schematic of the state transitions of the SAITS model.

The following dynamic equations can be obtained from the proposed model

$$\begin{aligned}
\frac{dS}{dt} &= rI - u_1(t)S - \beta_1 SI + \lambda T,\\
\frac{dA}{dt} &= u_1(t)S - \beta_2 AI,\\
\frac{dI}{dt} &= \beta_1 SI + \beta_2 AI - rI - u_2 I,\\
\frac{dT}{dt} &= u_2(t)I - \lambda T.
\end{aligned} \tag{2.1}$$

Denote $p_i^S(t)$, $p_i^A(t)$, $p_i^I(t)$, $p_i^T(t)$, $p_i^S(t)$, $p_i^A(t)$, $p_i^I(t)$, $p_i^T(t) \in [0, 1]$ as the probability of an individual i being susceptible, alert, infected and treated, respectively. It is clear that if the number of individuals is large enough, the average of the probabilities of all individuals in each state will be equal to the density of individuals in the corresponding state. The discrete-time mathematical model based on the microscopic Markov chain approach is thus proposed as

$$\begin{aligned}
p_i^S(t+1) &= (1 - u_1(t) - q_i^{SI}(t))p_i^S(t) + rp_i^I(t) + \lambda p_i^T(t),\\
p_i^A(t+1) &= (1 - q_i^{AI}(t))p_i^A(t) + u_1(t)p_i^S(t),\\
p_i^I(t+1) &= (1 - u_2(t) - r)p_i^I(t) + q_i^{SI}(t)p_i^S(t) + q_i^{AI}(t)p_i^A(t),\\
p_i^T(t+1) &= (1 - \lambda)p_i^T(t) + u_2(t)p_i^I(t),
\end{aligned} \tag{2.2}$$

where $q_i^{SI}(t) = 1 - \prod_{j \in N_i}(1 - \beta_1 p_j^I a_{ij}(t))$ and $q_i^{AI}(t) = 1 - \prod_{j \in N_i}(1 - \beta_2 p_j^I a_{ij}(t))$ represent the probability that a susceptible individual S or an alert individual A is infected by an adjacent infected individual, respectively.

When the states of the individual's neighbors are independent of each other and the infection rate is sufficiently small, under these two assumptions [22], we can deduce that

$$\begin{aligned}
q_i^{SI}(t) &\approx \sum_{j=1}^{N} \beta_1 p_j^I a_{ij}(t),\\
q_i^{AI}(t) &\approx \sum_{j=1}^{N} \beta_2 p_j^I a_{ij}(t).
\end{aligned} \tag{2.3}$$

The mean-field model can then be written as

$$\begin{aligned}
\dot{p}_i^S(t) &= (-u_1(t) - \sum_{j=1}^{N} \beta_1 p_j^I a_{ij}(t)) p_i^S(t) + r p_i^I(t) + \lambda p_i^T(t), \\
\dot{p}_i^A(t) &= -\sum_{j=1}^{N} \beta_2 p_j^I a_{ij}(t) p_i^A(t) + u_1(t) p_i^S(t), \\
\dot{p}_i^I(t) &= (-u_2(t) - r) p_i^I(t) + \sum_{j=1}^{N} \beta_1 p_j^I a_{ij}(t) p_i^S(t) + \sum_{j=1}^{N} \beta_2 p_j^I a_{ij}(t) p_i^A(t), \\
\dot{p}_i^T(t) &= -\lambda p_i^T(t) + u_2(t) p_i^I(t).
\end{aligned} \tag{2.4}$$

3. Theoretical analysis

3.1. Basic reproduction number

According to the method proposed in [23], the basic reproduction number of Eq (2.1) is calculated

$$R_0 = \rho(FV^{-1}) = \frac{\beta_1 + \beta_2}{u_2 + r}. \tag{3.1}$$

It can be seen that the propagation threshold R_0 is positively correlated with β_1 and β_2, and is negatively correlated with $u_2 + r$. Several sets of numerical simulation experiments are conducted to verify this conclusion, with the step of 0.2 and running 100 steps. The experimental results are shown in Figure 2. To make the results more accurate, the control variable method is utilized. When one variable is chosen for comparison, the other variables take the same values as the standard group. The parameters for the standard group are set as β_1= 0.30, β_2= 0.05, r= 0.10, λ= 0.50, u_1=u_2= 0.2.

As can be seen in Figure 2(a), the proportion of infected individuals increases as β_1 gets larger. Figure 2(b) shows that the proportion of infected individuals increases slightly as β_2 gets larger. Figure 2(c) shows that as r increases, the proportion of infected individuals decreases at the rate of 4%. Figure 2(d) indicates that as λ increases, there is nearly no change in the rising process while the stable value becomes progressively larger. Figure 2(e) shows that the rise time remains constant with u_1 increasing. Figure 2(f) indicates a large decrease in the stable value of the proportion of infected individuals with u_2 increasing. Based on the analysis above, the effect of β_2 on the proportion of infected individuals is the weakest, while the effect of u_2 is the strongest. The effect of r is nearly linear, and the effect of β_1 and λ is between the above two. From this, we can conclude that increasing the recovery rate in the population, for example, by researching specific drugs and increasing access to health care, is more important and more effective than reducing the infection rate.

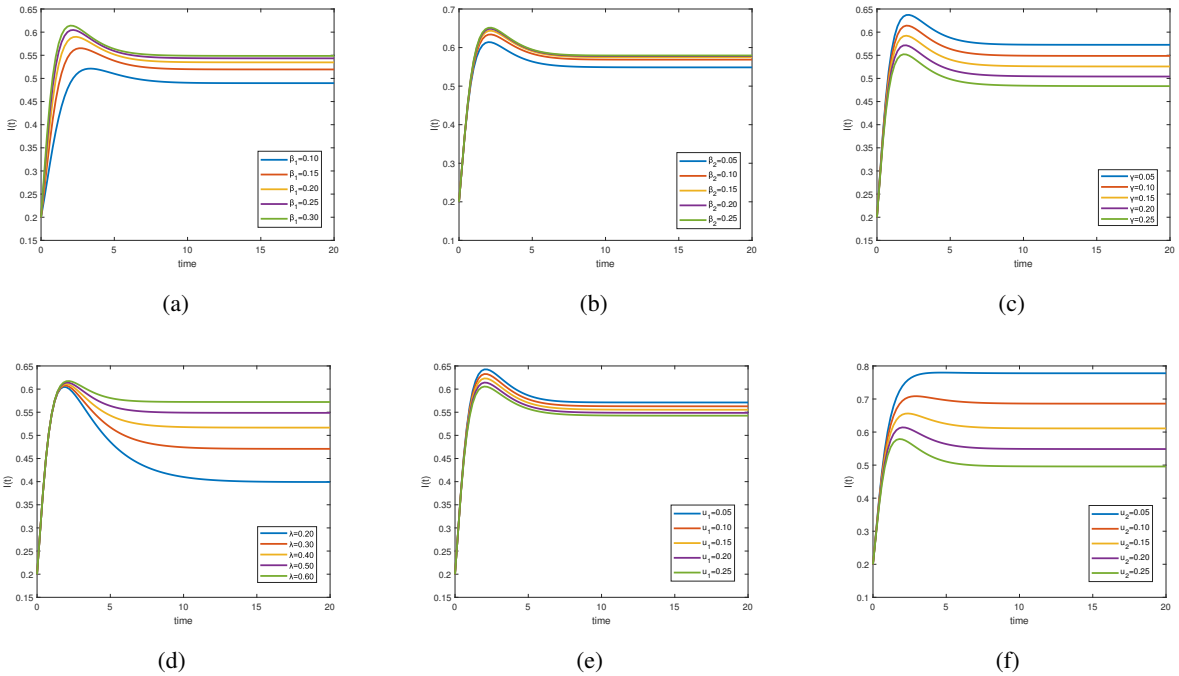

Figure 2. The time evolution of the fractions of infected individuals under different conditions. (a)–(f) are the change curves of $I(t)$ when β_1, β_2, r, λ, u_1 and u_2 are changed, respectively.

3.2. Combinational optimal suppression control

In this section, a global optimization problem is constructed to achieve the goal of global optimization by finding the optimal weighting coefficients in a combinational suppression control strategy. In the process of controlling infectious disease, on the one hand, there is a population infection cost, denoted as J_1, which is related to p_i^I, and on the other hand, there is a combinational optimal suppression control cost, denoted as J_2, which is determined by the control strategy proposed in Section 2. Thus, the objective function is the sum of these two kinds of costs for all individuals over the time interval $[0, T]$. We consider the cumulative cost over the entire time interval, that is, the total cost, denoted by J. The following is the procedure of solving the optimal solution in this time interval.

Based on the above discussion, the cost of the optimization problem is expressed as

$$J = \int_0^T (J_1 + J_2)dt, \tag{3.2}$$

where

$$J_1 = \sum_{i=1}^{N} d_i p_i^I(t),$$

$$J_2 = \frac{c_1}{2}u_1(t)^2 + \frac{c_2}{2}u_2(t)^2.$$

We use the Hamiltonian method to solve this optimal control problem. Obviously, the Lagrangian

function of the optimal problem is defined according to the objective Eq (3.2) as follows

$$L = \frac{c_1}{2}u_1(t)^2 + \frac{c_2}{2}u_2(t)^2 + \sum_{i=1}^{N} dp_i^I(t), \tag{3.3}$$

where c_1 and c_2 are the control strategy weighting factors and d is the infection cost factor.

The Pontryagin's maximum principle is used to solve the expression for optimal control. The Hamiltonian function is constructed by combining the state equation with the objective function by introducing the costate variables $\lambda(t) = (\lambda_1(t), \lambda_2(t), \lambda_3(t), \lambda_4(t))$, transforming the optimal control problem into a problem of solving the minimum of the Hamiltonian function.

Define the Hamiltonian function as follows

$$H = \frac{c_1}{2}u_1(t)^2 + \frac{c_2}{2}u_2(t)^2 + \sum_{i=1}^{N} d_i p_i^I(t) + \sum_{i=1}^{N}\left(\lambda_{1i}\dot{p}_i^S(t) + \lambda_{2i}\dot{p}_i^A(t) + \lambda_{3i}\dot{p}_i^I(t) + \lambda_{4i}\dot{p}_i^T(t)\right), \tag{3.4}$$

where the costate variables satisfy the condition that $\dot{\lambda}_{1i}=\frac{\partial H}{\partial p_i^S}$, $\dot{\lambda}_{2i}=\frac{\partial H}{\partial p_i^A}$, $\dot{\lambda}_{3i}=\frac{\partial H}{\partial p_i^I}$, $\dot{\lambda}_{4i}=\frac{\partial H}{\partial p_i^T}$. Substituting Eq (2.4) into Eq (3.5), we can derive the expression for the accompanying variables

$$\dot{\lambda} = A\lambda + B, \tag{3.5}$$

$$A = \begin{bmatrix} u_1(t) + \sum\limits_{j=1}^{N}\beta_1 p_j^I(t)a_{ij} & -u_1 & -\sum\limits_{j=1}^{N}\beta_2 p_j^I(t)a_{ij} & 0 \\ 0 & \sum\limits_{j=1}^{N}\beta_2 p_j^I(t)a_{ij} & -\sum\limits_{j=1}^{N}\beta_2 p_j^I(t)a_{ij} & 0 \\ -r + \sum\limits_{j=1}^{N}\beta_1 a_{ij}p_j^S(t) & \sum\limits_{j=1}^{N}\beta_2 a_{ij}p_j^A(t) & r + u_2 - \sum\limits_{j=1}^{N}\beta_2 a_{ij}p_j^A(t) - \sum\limits_{j=1}^{N}\beta_1 a_{ij}p_j^S(t) & -u_2 \\ -\lambda & 0 & 0 & \lambda \end{bmatrix}, \tag{3.6}$$

$$B = \begin{bmatrix} 0 \\ 0 \\ -d_i \\ 0 \end{bmatrix}. \tag{3.7}$$

The following conditions need to be satisfied when calculating the optimal solution

$$\begin{aligned} \tfrac{\partial H}{\partial u_1(t)} &= c_1 u_1(t) + \sum_{i=1}^{N}(\lambda_{2i} - \lambda_{1i})p_i^S(t), \\ \tfrac{\partial H}{\partial u_2(t)} &= c_2 u_2(t) + \sum_{i=1}^{N}(\lambda_{4i} - \lambda_{3i})p_i^I(t). \end{aligned} \tag{3.8}$$

Let $\frac{\partial H}{\partial u_i} = 0$, $i = 1, 2$, we can obtain the optimal weighted control at time t satisfying

$$\begin{aligned} \overset{*}{u}_1 &= \frac{\sum\limits_{i=1}^{N}(\lambda_{2i}-\lambda_{1i})p_i^S(t)}{c_1}, \\ \overset{*}{u}_2 &= \frac{\sum\limits_{i=1}^{N}(\lambda_{4i}-\lambda_{3i})p_i^I(t)}{c_2}. \end{aligned} \tag{3.9}$$

Considering the property of the control space, we have the optimal control in the compact notation

$$\begin{aligned} \overset{*}{u}_1 &= \min\left\{\max\left\{0, \frac{\sum_{i=1}^{N}(\lambda_{2i}-\lambda_{1i})p_i^S(t)}{c_1}\right\}, 1\right\}, \\ \overset{*}{u}_2 &= \min\left\{\max\left\{0, \frac{\sum_{i=1}^{N}(\lambda_{4i}-\lambda_{3i})p_i^I(t)}{c_2}\right\}, 1\right\}. \end{aligned} \tag{3.10}$$

4. Numerical experiments

In this section, to verify the results of the disease-free equilibrium, endemic equilibrium and optimal control problems, an undirected BA scale-free network consisting of 1000 nodes and 9908 edges is constructed, which obeys a power-law distribution $p_k = \sigma k^{-\upsilon}$. Specifically, k is defined as the degree of an individual, and the power-law exponent $\upsilon = 3.516$. The nodes in this network have a minimum degree $k_{\min} = 10$ and a maximum degree $k_{\max} = 172$. To be more realistic, u_1 is considered to have an initial value, since there is a certain proportion of individuals who can spontaneously switch from the S to the A, which is partly excluded from the cost calculation. In addition, u_2 has an initial value that fully accounts for the cost.

4.1. Disease-free and endemic equilibrium

With no additional control strategy, the initial proportion of individuals in S and I are set at 80% and 20% of the total population , and the initial value of control strategy are $u_1 = u_2 = 0.2$. Two scenarios are discussed below, by averaging 20 independent Monte Carlo simulations with the step of 0.2. For better comparison, different time scales are chosen for the Monte Carlo simulation and numerical simulation. In the first case, the former runs for 1500 steps and the latter for 1000 steps; in the second case, the former runs for 50 steps and the latter for 250 steps. The experimental results are shown in Figure 3.

For the first case, the parameters of the epidemic model are $\beta_1 = 0.50$, $\beta_2 = 0$, $r = 0.10$, $\lambda = 0.50$. When $\beta_2 = 0$, all individuals will eventually enter state A after a time. This deduction is shown in Figure 3(a),(b), which show the change of the population proportion in each compartment under Monte Carlo simulation and numerical simulation, respectively. It can be seen that the proportion of infected individuals dropped to zero, and the model reached a disease-free equilibrium.

For the second case, the parameters of the epidemic model are $\beta_1 = 0.30$, $\beta_2 = 0.10$, $r = 0.10$, $\lambda = 0.30$. Figure 3(c),(d) show the change of the population density in each state under Monte Carlo simulation and numerical simulation, respectively. As shown in these figures, an endemic equilibrium state is reached. The proportion of I and A in Figure 3(c) is slightly smaller than that in Figure 3(d), the proportion of S and T is slightly larger.

Figure 3 shows that the curves under Monte Carlo simulation rises and falls faster than that under numerical simulation with a large spike. When $\beta_2 = 0$, the system will reach a disease-free equilibrium, and when $\beta_2 \neq 0$, the system will enter an endemic equilibrium.

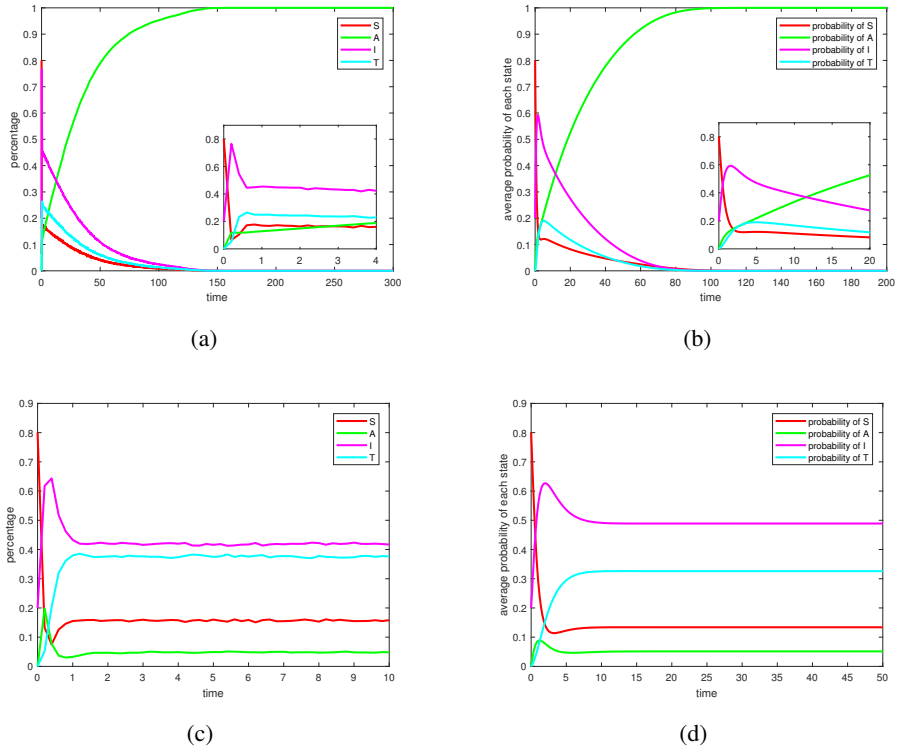

(a) (b)

(c) (d)

Figure 3. The proportion of individual in each compartment under different circumstances. (a) and (c) are the results under Monte Carlo simulation, and (b) and (d) are the results under numerical simulation.

4.2. Optimal control mechanism

To evaluate the performance of the combinational optimal suppression control mechanism proposed in Section 3.2, we introduce the following heuristic control strategy, where the range of c_1, c_2 is [0, 1],

$$u_1(t) = u_1(0) + c_1 p_i^S, u_2(t) = u_2(0) + c_2 p_i^I. \tag{4.1}$$

In this paper, we choose $c_1 = c_2 = 0.5$.

In Figure 4, we give comparative results of the cumulative cost, proportion of infected persons and control strategies for the same network under the respective actions of optimal control strategy, heuristic control strategy and no control strategy. Optimal control refers to the combinational optimal suppression control described in Section 3.2. All Monte Carlo simulation results are obtained by averaging 20 independent experiments, where the propagation parameters are β_1= 0.50, β_2= 0.05, r= 0.002, λ= 0.50, c_1=c_2= 10, d= 0.02 and $u_1 = 0.2$, $u_2 = 0.6$ are taken as the initial values of the control strategy. Experiments run 40 steps at the step of 0.05 and at this time, a steady state has been reached.

As can be seen in Figure 4(a), the total cost under the optimal control strategy is the lowest, and that under no control strategy is the highest. Due to the fact that the heuristic control seeks only the best control effect regardless of cost, as is shown in Figure 4(b),(c),(f), the heuristic control strategy has the fewest infected individuals and the highest control cost. For the optimal control, the control strategy u_2

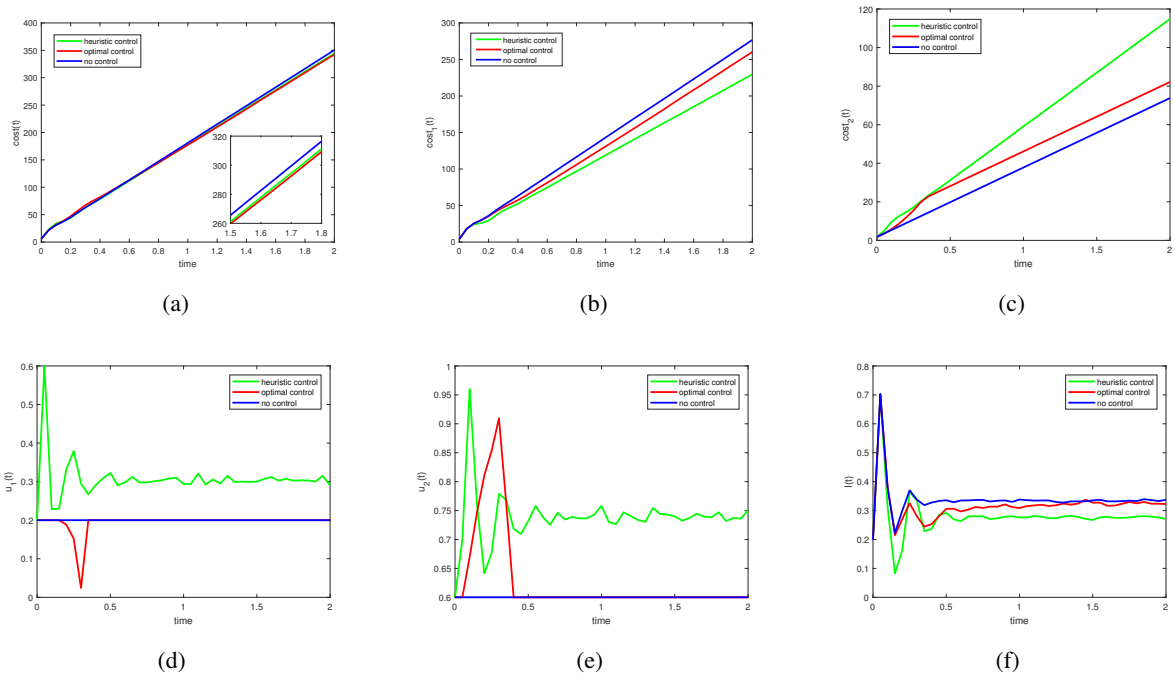

Figure 4. Comparison of experimental results under different control effects. (a) *cost* versus t (*cost* represents cumulative total cost). (b) $cost_1$ versus t ($cost_1$ represents cumulative infection cost). (c) $cost_2$ versus t ($cost_2$ represents cumulative control cost). (d) u_1 versus t. (e) u_2 versus t. (f) $I(t)$ versus t ($I(t)$ represents the population of infected individuals).

is only taken at the beginning of the outbreak of the disease in Figure 4(e), while the control strategy u_1 is slightly decreased in Figure 4(d). This is because it is more effective to use both strategies than either one alone, and improving the recovery rate is more effective than reducing the infection rate. To minimize the cost, the optimal control reduces the cost of the latter while increasing the cost of the former. Figure 4(c) shows that the optimal control strategy is stopped after the spread is suppressed, so its control cost is a little higher than no control strategy, but the curve is parallel to it as they all have initial control cost. It can be seen that both optimal control and heuristic control can suppress the spread of the disease. The heuristic is more costly, so its control effect is better. The optimal control strategy is more effective than other strategies at minimizing the total cost.

5. Conclusions

This paper presents the SAITS epidemic model with a combinational optimal suppression control strategy, which considers two measures to control the spread of the disease, moving more individuals to the compartment with low infection rate or the compartment with high recovery rate. The basic reproduction number of this model is calculated and the effect of each parameter on the outbreak threshold is discussed. It is found that increasing the recovery rate is more effective in suppressing the spread of the disease. We present an optimal problem with a trade-off in resource allocation considering the cost of the combinational optimal suppression control and global infection, and propose the structure of a general solution. A series of Monte Carlo simulations are performed to demonstrate the validity of the

theoretical results. The costs of three control strategies, optimal, heuristic and no control strategies, are compared, and the experimental results show that optimal control is more effective in minimizing costs compared with other control strategies.

Our work provides new explanations for the dynamics of epidemic transmission, and conclusions drawn from the optimal control problem may provide effective ways for governments or other organizations to suppress viral or other transmission processes.

Acknowledgments

This work was supported by the National Key Research and Development Program of China under Grant 2019YFE0118700 and the National Natural Science Foundation of China under Grant 61873194.

Conflict of interest

The authors declare there is no conflict of interest.

References

1. D. Chakrabarti, Y. Wang, C. Wang, J. Leskovec, C. Faloutsos, Epidemic thresholds in real networks, *ACM Trans. Inf. Syst. Secur.*, **10** (2008), 1–26. https://doi.org/10.1145/1284680.1284681
2. F. Di Lauro, J. C. Croix, M. Dashti, L. Berthouze, I. Z. Kiss, Network inference from population-level observation of epidemics, *Sci. Rep.*, **10** (2020), 18779. https://doi.org/10.1038/s41598-020-75558-9
3. Y. Zhao, C. Huepe, P. Romanczuk, Contagion dynamics in self-organized systems of self-propelled agents, *Sci. Rep.*, **12** (2022), 2588. https://doi.org/10.1038/s41598-022-06083-0
4. G. Albi, L. Pareschi, M. Zanella, Control with uncertain data of socially structured compartmental epidemic models, *J. Math. Bio.*, **82** (2021), 63. https://doi.org/10.1007/s00285-021-01617-y
5. J. M. Mendes, P. S. Coelho, Addressing hospitalisations with non-error-free data by generalised SEIR modelling of COVID-19 pandemic, *Sci. Rep.*, **11** (2021), 19617. https://doi.org/10.1038/s41598-021-98975-w
6. M. Shoaib, N. Anwar, I. Ahmad, S. Naz, A. K. Kiani, M. A. Z. Raja, Intelligent networks knacks for numerical treatment of nonlinear multi-delays SVEIR epidemic systems with vaccination, *Int. J. Mod. Phys. B*, **36** (2022). https://doi.org/10.1142/S0217979222501004
7. G. Albi, L. Pareschi, M. Zanella, Modelling lockdown measures in epidemic outbreaks using selective socio-economic containment with uncertainty, *Math. Biosci. Eng.*, **18** (2021), 7161–7190. https://doi.org/10.3934/mbe.2021355
8. P. Di Giamberardino, D. Iacoviello, Evaluation of the effect of different policies in the containment of epidemic spreads for the COVID-19 case, *Biomed. Signal Process. Control*, **65** (2021), 102325. https://doi.org/10.1016/j.bspc.2020.102325
9. K. M. A. Kabir, K. Kuga, J. Tanimoto, Effect of information spreading to suppress the disease contagion on the epidemic vaccination game, *Chaos, Solitons Fractals*, **119** (2019), 180–187. https://doi.org/10.1016/j.chaos.2018.12.023

10. X. Wang, D. Jia, S. Gao, C. Xia, X. Li, Z. Wang, Vaccination behavior by coupling the epidemic spreading with the human decision under the game theory, *Appl. Math. Comput.*, **380** (2020), 125232. https://doi.org/10.1016/j.amc.2020.125232
11. M. Chinazzi, J. T. Davis, M. Ajelli, C. Gioannini, M. Litvinova, S. Merler, et al., The effect of travel restrictions on the spread of the 2019 novel coronavirus (COVID-19) outbreak, *Science*, **368** (2020), 395–400. https://doi.org/10.1126/science.aba9757
12. S. Kwon, A. D. Joshi, C. Lo, D. A. Drew, L. H. Nguyen, C. Guo, et al., Association of social distancing and face mask use with risk of COVID-19, *Nat. Commun.*, **12** (2021), 3737. https://doi.org/10.1038/s41467-021-24115-7
13. H. Shi, Z. Duan, G. Chen, R. Li, Epidemic spreading on networks with vaccination, *Chin. Phys. B*, **18** (2009), 3309–3317. https://doi.org/10.1088/1674-1056/18/8/035
14. A. S. Alsheri, A. A. Alraeza, M. R. Afia, Mathematical modeling of the effect of quarantine rate on controlling the infection of COVID19 in the population of Saudi Arabia, *Alexandria Eng. J.*, **61** (2022), 6843–6850. https://doi.org/10.1016/j.aej.2021.12.033
15. D. Xu, X. Xu, Y. Xie, C. Yang, Optimal control of an SIVRS epidemic spreading model with virus variation based on complex networks, *Commun. Nonlinear Sci. Numer. Simul.*, **48** (2017), 200–210. https://doi.org/10.1016/j.cnsns.2016.12.025
16. A. P. Lemos-Paião, C. J. Silva, D. F. M. Torres, An epidemic model for cholera with optimal control treatment, *J. Comput. Appl. Math.*, **318** (2017), 168–180. https://doi.org/10.1016/j.cam.2016.11.002
17. L. Miclo, D. Spiro, J. Weibull, Optimal epidemic suppression under an ICU constraint: An analytical solution, *J. Math. Econ.*, **101** (2022), 102669. https://doi.org/10.1016/j.jmateco.2022.102669
18. Y. Wu, Y. Sun, M. Lin, SQEIR: An epidemic virus spread analysis and prediction model, *Comput. Electr. Eng.*, **102** (2022), 108230. https://doi.org/10.1016/j.compeleceng.2022.108230
19. A. Kumar, P. K. Srivastava, Y. Dong, Y. Takeuchi, Optimal control of infectious disease: Information-induced vaccination and limited treatment, *Phys. A: Stat. Mech. Appl.*, **542** (2020), 123196. https://doi.org/10.1016/j.physa.2019.123196
20. G. Dimarco, G. Toscani, M. Zanella, Optimal control of epidemic spreading in the presence of social heterogeneity, *Philos. Trans. R. Soc. A*, **380** (2022), 2224. https://doi.org/10.1098/rsta.2021.0160
21. G. Zaman, Y. Kang, G. Cho, I. H. Jung, Optimal strategy of vaccination & treatment in an SIR epidemic model, *Math. Comput. Simul.*, **136** (2017), 63–77. https://doi.org/10.1016/j.matcom.2016.11.010
22. Y. Pan, Z. Yan, The impact of individual heterogeneity on the coupled awareness-epidemic dynamics in multiplex networks, *Chaos*, **28** (2018), 063123. https://doi.org/10.1063/1.5000280

23. P. van den Driessche, J. Watmough, Reproduction numbers and sub-threshold endemic equilibria for compartmental models of disease transmission, *Math. Biosci.*, **180** (2002), 29–48. https://doi.org/10.1016/S0025-5564(02)00108-6

AIMS Press